Parametrization of electronic band structure using the Green's-function method: Empirical application to Cu and Ag†

An-Ban Chen* and Benjamin Segall
Department of Physics, Case Western Reserve University, Cleveland, Ohio 44106
(Received 23 September 1974)

A new empirical energy-band parametrization scheme based on the Green's-function method has been developed and was applied to Cu and Ag. The scheme utilizes the logarithmic derivatives associated with an *ab initio* muffin-tin potential $V^{(0)}(r)$. The scheme can be understood in terms of the addition to $V^{(0)}$ of E- and l-dependent square-well potentials the depths of which $v_l(E)$ are adjusted to yield the correct (empirical) energy bands. The $v_l(E)$ are found to be smooth functions of E which can be accurately approximated by low-order polynomials. An accurate fit for d-band metals over a roughly 1-Ry range requires only seven adjustable parameters — a number smaller than required by other schemes. Extensive tests of the approach using results of first-principles calculations were carried out in precisely the same manner as proposed for the empirical application, and the results indicate that this scheme is more accurate than other approaches using more parameters. The seven pieces of data used in the empirical parametrization for Cu and Ag were the s, p, and d phase shifts required to fit the Fermi-surface geometry and four firmly identified vertical energy gaps: $E_F - X_5$, $X_4' - X_5$, $X_5 - X_3$, and $L_1^u - L_2'$. The empirical $E_n(\vec{k})$ were obtained for a large range of E_F values (relative to the constant part of the potential). Except for the rather high energy levels (e.g., the upper X, W, and K states) the relative band structures prove to be rather insensitive to the E_F value. The presently available and firmly established data do not narrow the permissible range of E_F. Comparisons with several recent Cu and Ag calculations show that the present bands are in better accord with experiments. The empirical $E_n(\vec{k})$, which are required to fit the input data, are also found to agree within experimental uncertainties with all additional data related to level positions. Cu, for which more data are available, is particularly well checked. To obtain some information about the effective interactions $V_l(E,r)$ and the associated wave functions, a set of coupled integro-differential equations is derived which relates these quantities to the $v_l(E)$. However, it appears that the solutions to these equations are not unique unless some constraints are imposed on the correction $V_l(E,r) - V^{(0)}(r)$. A suggestion is made for obtaining approximate useful wave functions prior to the resolution of the nonuniqueness problem. From our experiences and a consideration of the merits of the new scheme, it is evident that it should be very useful in the study of the electronic structure of various solids.

I. INTRODUCTION

For over a decade there has been considerable interest in the development of parametrization schemes[1-5] for electronic band structures. Since these schemes can be used with different goals in mind and in different ways it is useful to state our orientation at the outset. Often these schemes have been used to provide a more economical means for computing the $E_n(\vec{k})$ than the standard band methods. Though this is a valid purpose, it is not the one we are primarily concerned with. Our goal is to obtain an accurate description of the electronic structures and in the process some information about the effective potential using empirical data. We adopt this point of view because we believe that, at the present time, it is not possible to consistently construct *a priori* potentials which yield quantitatively accurate excitation spectra. For one thing, we do not have an accurate way of incorporating many-electron contributions. Thus, we take a frankly empirical approach in which we effectively allow the data to determine the spectra over the range of interest.

We note that there is a different approach than ours which is in effect a parametrization approach, although it is generally not referred to as such. This involves the calculation of the $E_n(\vec{k})$ for a variety of potentials including variable exchange-correlation contributions (e.g., the $X\alpha$ recipe) and the subsequent determination of the potential which leads to the best agreement with experiment. However, we feel that a more fully empirical approach of the type we have in mind is generally less restrictive in regard to the possible interactions and should allow for a more detailed fitting of the data.

The particular solids that we have investigated are Cu and Ag. These metals are ideal subjects for such a study since their energy-band structures and the bodies of data relating to them are relatively rich.

The parametrization scheme that we use is based on the Green's function method (GFM),[6] which is also known as the Korringa-Kohn-Rostoker (KKR) method.[7] The use of the GFM as the basis of such an approach was first suggested by Segall and Ham.[6] In the GFM the $E_n(\vec{k})$ are obtained

from the determinantal equations

$$\det[B_{lm,l'm'}(E,\vec{k})+\delta_{ll'}\,\delta_{mm'}E^{1/2}\cot\eta_l(E)]=0\,. \tag{1}$$

In Eq. (1) the effect of potential is completely contained in the $\cot\eta_l(E)$ term—or, equivalently, in the logarithmic derivative $\mathcal{L}_l(E)$. Since in practice only $l\leq 2$ components are required to obtain highly accurate $E_n(\vec{k})$ for crystals for which the muffin-tin approximation is useful, it is only necessary to parametrize the $\eta_l(E)$, or the $\mathcal{L}_l(E)$, for the lowest three l values. It is useful to remark that the class of potential operators leading to Eq. (1) includes l- and E-dependent muffin-tin potentials as well as simple local functions. Thus the interactions encompassed by the parametrization scheme include these more general potentials.

The use of the GFM in the parametrization of Fermi-surface data has been successfully implemented by Shaw *et al.*[8] in their work on the noble metals. The first GFM parametrization of the energy bands over a broad energy range, roughly 1 Ry centered approximately at the Fermi energy E_F, was carried out for the noble metals by Cooper, Kreiger, and Segall[4] (CKS). In this work the potential-dependent terms that were parametrized were the $\tan\eta_l(E)$. More recently, Chen *et al.*[5] (to be referred to as I) considered two schemes which were based primarily on the $\mathcal{L}_l(E)$. One of these proved to be a distinct improvement over other parametrization schemes. For a d-band metal, this approach required nine adjustable parameters and yielded extremely accurate eigenvalues. In fact, the errors in the $E_n(\vec{k})$ (~ 0.001 Ry) were much smaller than the uncertainties in many of the experimental data. (The uncertainties in the optical gaps are generally 0.1 eV or larger.) This suggested that the number of parameters could be reduced. This would be a desirable accomplishment, since the amount of useful independent data for our purposes over the energy range of interest are not great, even for such thoroughly studied metals as Cu and Ag. As will be clear later, nine is still too large a number of parameters for what will loosely be called a "fully empirical"[9] parametrization.

At this point it is useful to note that though the potential dependent quantities [e.g., the $\mathcal{L}_l(E)$] obtained in a first-principles calculation are not as quantitatively accurate as desired—if they were, there would be no need for empirical schemes—they do not differ appreciably from the correct, or empirical, functions. We certainly expect the calculated energy dependences to be essentially correct. In the previous work we used the first-principles results to suggest functional forms and for testing purposes. However, we feel that the considerable information contained in the calculated results has not been effectively exploited. In this paper we develop a new scheme which is based on the *ab initio* results but which has the necessary flexibility for adjustments required in an empirical parametrization. In effect, the new scheme consists of using the calculated values of $\mathcal{L}_l(E)$ but with a shifted and distorted energy scale. This is effected by replacing the independent variable E by $E+v_l(E)$ for each l value. This is equivalent to adding an l- and E-dependent square-well potential to the potential used in the first-principles calculation. The $v_l(E)$ are the quantities to be parametrized. For a monatomic d-band metal, it turns out that only seven adjustable parameters are required for an accurate fit of the energy bands over a 1-Ry range. This, we believe, is substantially better than other schemes that have been proposed. Also, this relatively small number permits us to undertake the type of empirical application to Cu and Ag that we have in mind.[9]

As emphasized earlier,[4-6] the basic quantities employed in a scheme based on the GFM (the $\mathcal{L}_l$ or $\tan\eta_l$), in contrast to those used in many other approaches, are directly related to the solutions of the effective one-electron Schrödinger equation. They are thereby related in a clear-cut way to the effective interaction operator $\hat{V}$. In this paper we pursue this matter further. A set of equations is derived which relate the $v_l(E)$ (or the corrections to the *ab initio* logarithmic derivatives) to the potential correction $\delta\hat{V}=\hat{V}-\hat{V}^{(0)}$ and the associated radial functions for $\hat{V}$, where $\hat{V}^{(0)}$ is the reference *ab initio* potential. The matter of the nonuniqueness of the solutions to these equations is considered as is the question of obtaining approximate wave functions.

In Sec. II we discuss the new parametrization scheme. Using several different first-principles calculations for Cu and Ag, we demonstrate the practicality of the new approach. In Sec. III we discuss the empirical data to be used in the application to Cu and Ag. The detailed procedures by which the $\mathcal{L}_l(E)$, and thus the $v_l(E)$ are determined from the data are given in Sec. IV. It is, of course, of considerable importance to have a reliable measure of the accuracy of schemes of the general type we are considering. We note that the accuracy of a scheme is dependent on the manner in which the parameters are determined, in particular on the energies at which they are determined. In an empirical application of the type we are concerned with, one has limited freedom

to choose these energies. We have thus made tests of our approach using the results from several *a priori* calculations. These tests are carried out in Sec. V in precisely the same manner as proposed for the fully empirical application. The empirical parametrization for Cu and Ag is carried out in Sec. VI. In Sec. VII the band structures for Cu and Ag associated with the empirically determined $\mathcal{L}_l(E)$ are discussed and comparisons are made with several previous calculations and with available data. In Sec. VIII we consider the relations connecting the $\delta\hat{V}$, the radial wave functions, and the $v_l(E)$. Section IX contains a summary and conclusions.

II. NEW PARAMETRIZATION SCHEME

As we noted above, the accuracy of the more accurate scheme in I was much higher than required by many of the present data. This suggested that with perhaps some relaxation in the accuracy we might be able to reduce the number of adjustable parameters. The desirability of that goal was emphasized in Sec. I. Also, it was evident that the approach in I did not utilize to any great extent the valuable information contained in the logarithmic derivatives of a reasonably good first-principles calculation. On the basis of the fair success of band calculations in recent years, it is clear that the calculated logarithmic derivatives which we will denote $\mathcal{L}_l^{(0)}(E)$, are, at least, semiquantitatively accurate. Certainly, the essential features of the energy dependences are given correctly by these functions. The only problem is that these functions are not as quantitatively precise as we presently desire.[10] One can easily envision that with some small shifts and distortions these $\mathcal{L}^{(0)}(E)$ curves could be made to match the correct $\mathcal{L}_l(E)$.

As already noted in I, for a d-band metal the most critical and most difficult potential-dependent term is that for $l=2$ in the d-band region. The most sensitive aspect of the $\mathcal{L}_2(E)$ is the location of the singularity (which is close to the so-called d resonance, or pole, of $\tan\eta_2$) and the shape of the function in its vicinity. These features are the essential determinants for the $E(\vec{k})$ in the d-band region. From our experience, it seems evident that the envisioned shift and small distortion of $\mathcal{L}_2^{(0)}(E)$ should be sufficient to correct this relatively difficult quantity.

It turns out that it is rather simple to implement this goal. We propose that the desired logarithmic derivatives be represented by

$$\mathcal{L}_l(E) = \mathcal{L}_l^{(0)}(E + v_l(E)) , \tag{2}$$

where the functions $v_l(E)$ depend on l. A constant v_l just provides a rigid shift of the original $\mathcal{L}_l^{(0)}(E)$, while an energy dependence leads to the distortion. For the approach to be practical, the $v_l(E)$ must be relatively smoothly varying functions of E. This will be demonstrated below.

Another way of viewing the transformation in Eq. (2) is to note that it corresponds to the addition of an l- and E-dependent square-well potential $-v_l(E)$ to the *ab initio* $V_l^{(0)}(r)$. If the radial wave function for $V^{(0)}(r)$ is $R_l^{(0)}(E,r)$ for energy E, then the solution for the l- and E-dependent potential $\tilde{V}_l(E,r) = V^{(0)}(r) - v_l(E)$ is $R_l^{(0)}(E + v_l(E))$. [The original potential $V^{(0)}(r)$ need not be independent of l and E.] The logarithmic derivative for the modified potential is that given by Eq. (2). Conversely, any set of $\mathcal{L}_l(E)$ related to the $\mathcal{L}_l^{(0)}(E)$ by Eq. (2) can be produced by the potential $\tilde{V}_l(E,r)$, although this will not be a unique solution of the "inverse" problem [i.e., the determination of the potentials that lead to the given $\mathcal{L}_l(E)$, or the $\tan\eta_l(E)$].

It is useful to point out that Eq. (2) establishes a unique $v_l(E)$. To do this we utilize the fact, familiar from experience (see, for example, Fig. 1 of I), that the logarithmic derivative decreases monotonically from a positive-infinite to a negative-infinite value. The energy derivative of $\mathcal{L}_l$ can be derived by obtaining in the standard way the Wronskian for two radial functions $R_l(E,r) = r^{-1}P_l(E,r)$ for energies E and $E+\delta E$. The integral of the Wronskian then leads to

$$\frac{d\mathcal{L}_l}{dE} = -P_l^{-2}(E,r_i)\int_0^{r_i}\left(1 - \frac{\partial V_l(E,r)}{\partial E}\right)P_l^2(E,r)\,dr , \tag{3}$$

where $V_l(E,r)$ is the effective potential and r_i is the radius of the inscribed sphere. For a potential which is independent of E, Eq. (3) reduces to a well-known result[11] and the monotonicity is verified. Most potentials used in band calculations are of this type, so that the $\mathcal{L}_l^{(0)}(E)$ is monotone.[12] This fact ensures that $v_l(E)$ is determined uniquely by Eq. (2). To ascertain the behavior of the derivative of the empirical $\mathcal{L}_l(E)$ it is necessary to know something about $\partial V/\partial E$. Further discussion of this will be deferred until Sec. VII.

To investigate the behavior of the $v_l(E)$, we have made comparisons between the $\mathcal{L}_l$ for quite different potentials for the same metal using the results from first-principles calculations for Cu and Ag. Explicitly, we took two sets of $\mathcal{L}_l$ denoted by $\mathcal{L}_l^A(E)$ and $\mathcal{L}_l^B(E)$ corresponding to two different potentials V_A and V_B and related them by

$$\mathcal{L}_l^A(E) = \mathcal{L}_l^B(E + v_l(E)) . \tag{2'}$$

The functions $v_l(E)$ were then determined. These are plotted in Fig. 1 for two pairs of Cu potentials.

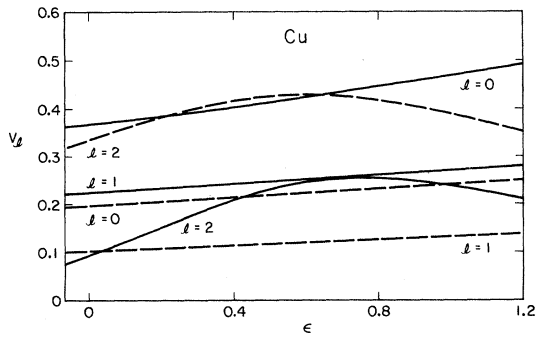

FIG. 1. $v_l(E)$ for $l \leq 2$ corresponding to two pairs of *ab initio* lagarithmic derivatives for Cu. The v_l and E are in crystal units. For the solid and dashed curves the $\mathcal{L}_l^B(E)$ in Eq. (2′) are, respectively, the logarithmic derivatives for the so-called l-dependent and Cu($\frac{2}{3}$) potentials, while the $\mathcal{L}_l^A(E)$ in both cases are for the Chodorow potential. (See text for the notations for the potentials.)

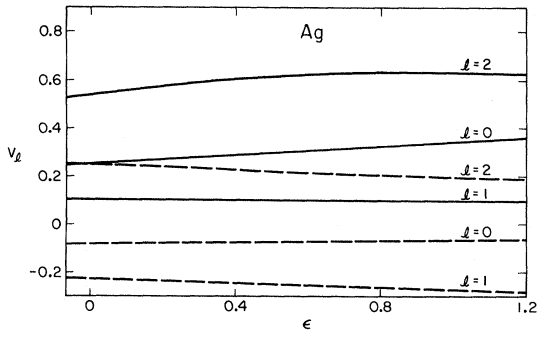

FIG. 2. $v_l(E)$ for $l \leq 2$ corresponding to two pairs of *ab initio* logarithms derivatives for Ag. The v_l and E are in crystal units. For the solid and dashed curves the $\mathcal{L}_l^{(B)}(E)$ in Eq. (2′) are, respectively, the logarithmic derivatives for the so-called Ag($\frac{2}{3}$) and Ag(H) potentials, while the $\mathcal{L}_l^A(E)$ in both cases are for the Ag(HF) potential. (See text for the notations for the potentials.)

The solid curves are the $v_l(E)$ for $l=0$, 1, and 2 with V_A and V_B being the so-called Chodorow[13,14] and l-dependent potentials,[13] respectively. The dashed curves are the $v_l(E)$ corresponding to V_A being the Chodorow potential and V_B being what we will call the Cu($\frac{2}{3}$) potential. The latter potential is constructed by the usual procedure of superposing atomic potentials and charge densities[15] and using the local exchange contribution with the exchange coefficient $\alpha = \frac{2}{3}$. We note that v_0 and v_1 are quite accurately linear functions of E. The v_2 are very smooth functions which we found could be accurately approximated by a quadratic function of E. In Fig. 2 the corresponding v_l are plotted for two pairs of Ag potentials. For the dashed curves the $\mathcal{L}_l^A$ and $\mathcal{L}_l^B$ correspond to what have been called the Ag(HF) (Hartree-Fock) and Ag(H) (Hartree) potentials, respectively.[4,16] For the solid curves, the $\mathcal{L}_l^A$ are for the Ag(HF) potential, while the $\mathcal{L}_l^B$ correspond to the Ag($\frac{2}{3}$) potential, which is obtained in the same way as the Cu($\frac{2}{3}$) potential. Again the v_0 and v_1 are accurately represented by straight lines, while the v_2 are even smoother functions than those in Fig. 1 for Cu.

These results strongly support our expectations about the efficacy of the scheme, namely, that the $\mathcal{L}_l(E)$ can be conveniently parametrized via the $v_l(E)$. It is clear that for the energy range considered the three $v_l(E)$ can be accurately represented by the three simple polynomials

$$v_0(E) = S_0 + S_1 E\,, \tag{4a}$$

$$v_1(E) = P_0 + P_1 E\,, \tag{4b}$$

$$v_2(E) = D_0 + D_1 E + D_2 E^2\,. \tag{4c}$$

The seven coefficients appearing in Eqs. (4) are the adjustable parameters of our scheme. They must be determined by seven pieces of empirical data.

III. INPUT DATA

Since a major goal of this work is the empirical parametrization of Cu and Ag, the choices of the nature and amount of the data as well as the specific values are of paramount importance. Several criteria were imposed on the selection of data. These were as follows: (i) The interpretation of the data (e.g., the identification of an optical gap) should be unambiguous; (ii) the data should be known with reasonable precision; (iii) the data are suitably distributed over the energy range of interest; (iv) the data are sufficiently independent in regard to their relationship to the $\mathcal{L}_l(E)$; (v) the data are reasonably convenient to use to determine the $v_l(E)$. Requirements (i), (ii), and (v) need no explanation. The requirements for the distribution of the data, (iii), are different for the different l. As emphasized earlier, it is important that the $\mathcal{L}_2(E)$ be determined accurately in the d-band region. This necessitates at least two pieces of data in that region which, we might picture, suffices to locate the d resonance and to fix its width. Another datum outside (above) the d-band region is needed to determine the nonresonance contribution to $\mathcal{L}_2(E)$. On the other hand, the energy range of most importance for the s and p terms are at and above E_F.[17] In regard to (iv) we give an example of data which would not be sufficiently independent: the Fermi-surface data leading to the $\mathcal{L}_1(E_F)$ and the location of the $L_{2'}$ state relative to E_F which determines $\mathcal{L}_1$ at $E(L_{2'})$. For Ag, $E_F - E(L_{2'}) \approx 0.3$ eV, so that

these two pieces of information about $\mathcal{L}_1(E)$ are almost redundant.[18]

After surveying the available data, we concluded that there are seven pieces of data that generally satisfy the above criteria. Of these seven, three relate to the Fermi surface. These data are very useful because of their accuracy and because they fall in the middle of the energy range of interest. Since the Fermi-surface data for the noble metals have already been fitted very precisely using the GFM by Shaw *et al.*,[8] we can directly use their results [i.e., the three $\eta_l(E_F)$] as "data" for our work. We recall that they were able to fit the data over a wide range of E_F values relative to the constant part of the muffin-tin potential, V_c. The values of $\eta_l(E_F)$ are given in Table I for five values of E_F for both metals.[19] The accuracies[8] of the $\eta_l(E)$'s are such that the deviations between the calculated and measured cross-sectional areas are of the order of one part in 10^4.

The other four pieces of data that we use for each metal are the energy gaps $L_1^u - L_2'$, $X_4' - X_5$, $E_F - d(\text{top})$, and $X_5 - X_3$. The values for the last gap, which essentially gives the widths of the d bands, have been obtained from the photoemission data of Eastman and Cashion.[20] The quoted uncertainty in these values are 0.3 eV, which is larger than those for the other gaps and makes this gap (and ultimately the locations of X_3) the most imprecisely known data we use. The other three gaps mentioned above have been identified in the past from the structure in $\epsilon_2(\omega)$. While $\epsilon_2(\omega)$ is certainly useful in identifying transitions, it has some shortcomings. These are (a) $\epsilon_2(\omega)$ involves contributions from the complete Brillouin zone and all appropriately occupied bands, which makes the identification of some transitions less than unambiguous, and (b) the structure is not especially sharp or well defined (in part because of overlapping contributions), making the determination of the gaps less accurate than desired. We note that much more definitive identifications of transitions and accurate determinations are possible if single-crystal piezo-optical data are available, as is the case for[21] Cu and[22] Ag.

TABLE I. Empirical data used in the band-structure parametrization of Cu and Ag. The phase shifts are obtained from Ref. 8 (see also the comment in Ref. 19). The justification for the values of the energy gaps are given in Sec. III of the text.

	E_F[a]	η_0	η_1	η_2
Cu	0.9	−0.275 21	−0.052 55	−0.229 44
	0.8	−0.146 37	−0.023 88	−0.182 71
	0.690 398	0.006 70	0.100 73	−0.135 76
	0.45	0.422 59	0.225 47	−0.054 97
	0.3	0.764 57	0.234 13	−0.021 89
Ag	0.9	−0.195 26	−0.082 71	−0.222 79
	0.8	−0.067 21	−0.000 72	−0.176 16
	0.75	0.000 276	0.029 13	−0.154 35
	0.5	0.410 08	0.176 70	−0.065 09
	0.35	0.725 74	0.213 24	−0.029 01

Energy gap[b]	$E_F - X_5$	$X_4' - X_5$	$L_1^u - L_2'$	$X_5 - X_3$
Cu	−1.96	3.86	5.04	3.00
Ag	−3.81	5.65	4.23	3.50

[a] In crystal units (c.u.), i.e., $E(\text{Ry}) = \epsilon(\text{c.u.}) \times 4\pi^2/a^2$, where a is the lattice constant in a.u. The values of a used are 6.8090 and 7.6897 a.u. for Cu and Ag, respectively.

[b] In eV.

An analysis of the piezo-optical response functions of these metals[23] (to appear elsewhere) has yielded what we believe to be unambiguous identifications of the $d(\text{top}) \to E_F$ and $L_2' \to L_1^u$ transitions in both Cu and Ag and the $X_5 \to X_4'$ transitions in Cu, and also the most accurate determination of the transition energies. The corresponding gaps are given in Table I. The tabulated quantities connected with the $d(\text{top}) \to E_F$ transitions are the $E_F - X_5$ gaps. For Cu this is obtained from the 2.10-eV threshold corresponding to $\Delta_5 \to \Delta_1(E_F)$ and the small $X_5 - \Delta_5(k_F)$ correction taken from an *a priori* calculation. For Ag the tabulated value is obtained from the 4.1-eV $Q_+ \to Q_-(E_F)$ peak obtained from the isotropic response function and the $X_5 - Q_+(k_F)$ correction from a calculation. The possible error in using the calculated correction values is very small (< 0.05 eV).

The $X_4' - X_5$ separation for Ag was the only gap, aside from the d-band width, that could not be obtained from the piezo-optical spectra since it was outside the range of the data. For this gap we used the structure in $\epsilon_2(\omega)$ at 5.65 eV.[24] However, we believe that there are a few cogent arguments which firmly support this identification.[25] We estimate that the uncertainties in the optical gaps are about 0.1 eV, with the exception of the Ag $X_4' - X_5$ gap, for which it is 0.15 eV.

It is evident that the data mentioned above satisfy conditions (i)–(iv). That (v) is satisfied will be demonstrated in Sec. IV. We note that the locations of the X_5 and X_3 levels supply the required d-band information. If it were possible, it would be desirable to have the third $l = 2$ datum at an energy above E_F. The only candidate for this is the position of the L_1^u level, but this is used to determine $v_0(E)$. If this level were used for the d component, there would be no adequate means of determining the $v_0(E)$ over any range and, in particular, for $E \geq E_F$.[17]

There are other data which do not satisfy our

criteria and which we do not use as input data. These will be used as checks on the electronic structure that results from the empirical parametrization.

IV. PROCEDURE FOR DETERMINING v_l FROM DATA

The manner in which the parameters in Eq. (4) are determined is generally similar to the procedure employed in CKS. The details, however, are different because different sets of input data are used in the two investigations. In this section we enumerate in detail the steps that we employ in the empirical application to Cu and Ag. The steps below are carried out for a given value of E_F.

(a) As we noted in Sec. III, the phase shifts at $E=E_F$ have already been determined. It is merely necessary to obtain the $\mathcal{L}_l(E_F)$ from

$$\mathcal{L}_l(E)=\frac{j_l'(\kappa r_i)-n_l(\kappa r_i)\tan\eta_l(E)}{j_l(\kappa r_i)-n_l(\kappa r_i)\tan\eta_l(E)}\ , \tag{5}$$

where the j_l and n_l are the Bessel and Neumann functions, respectively, and $\kappa^2=E$. The values of the $v_l(E_F)$ are then determined using Eq. (2).

In the remaining steps we use the location of a given state, $E_n(\vec{k})$, to determine the $\mathcal{L}_l(E)$ and thus the $v_l(E)$. This procedure is simplified by the fact that our data pertain to states of high symmetry at which the left-hand side of Eq. (1) reduces to the determinant of a 1×1 or a 2×2 matrix for the truncation $l_{\max}=2$. Such equations can easily be inverted to obtain the $\tan\eta_l$ at known energies.

(b) The E_F-X_5 gap locates the position of the X_5 state. From the equation for X_5,

$$B_{21,21}+E^{1/2}\cot\eta_2=0\ , \tag{6}$$

the η_2 and the v_2 are determined at this energy.

(c) The $X_4'-X_5$ optical gap locates the position of the X_4' state. With the equation for this state,

$$B_{10,10}+E^{1/2}\cot\eta_1=0\ , \tag{7}$$

we determine the η_1 and then the v_1 at $E(X_4')$. This information along with the v_1 at E_F [step (a)] determines the two parameters P_0 and P_1 and thus completes the $l=1$ parametrization.

(d) The data on the d-band width, i.e., X_5-X_3, provide us with $E(X_3)$. The η_2 and the v_2 at $E(X_3)$ are then determined from the equation

$$B_{22,22}+E^{1/2}\cot\eta_2=0\ . \tag{8}$$

Since v_2 is also known at E_F [step (a)] and at $E(X_5)$ [step (b)], there is sufficient information to solve Eq. (4c) for D_0, D_1, and D_2. This then completes the parametrization of $v_2(E)$.

(e) The parametrized $v_1(E)$ [and thus the $\mathcal{L}_1(E)$] obtained in step (c) can be used in the equation for the L_2' level,

$$B_{10,10}+E^{1/2}\cot\eta_1=0\ , \tag{9}$$

to find the $E(L_2')$. The optical gap $L_1^u-L_2'$ locates the L_1^u state. The energy of this state satisfies

$$\det\begin{vmatrix} B_{00,00}+E^{1/2}\cot\eta_0 & B_{00,20} \\ B_{20,00} & B_{20,20}+E^{1/2}\cot\eta_2 \end{vmatrix}=0\ . \tag{10}$$

Since the $l=2$ parametrization has been completed in the previous step the η_2 is known at $E(L_1^u)$. The only unknown in Eq. (10) is η_0 at $E(L_1^u)$, and the equation is readily solved for this quantity. This value along with η_0 at E_F [step (a)] determines the S_0 and S_1 in Eq. (4a) and completes the parametrization procedure.

V. REALISTIC TESTS OF SCHEME

In the above procedure, the $v_l(E)$ are determined at a few energies in a restricted region dictated by the data employed. For example, the energies used to determine the v_2 are at and below E_F, while those used for the v_0 determination are at and above E_F. It would, of course, be desirable to fit the v_2 both above and below E_F, but, as pointed out in Sec. III, the data set does not permit this. In other studies, tests of the proposed schemes were made by setting conditions on the parametrized quantities at a generally optimally distributed set of energies. The resulting $E_n(\vec{k})$ were then compared with the results of *a priori* calculations. It is important to note that the errors recorded in such tests would generally be lower than the errors that would occur in an empirical (or semiempirical) application, where the energies for the input data are not open to choice. For this reason it is very important to assess the accuracy of the scheme in precisely the *same* manner planned for the empirical application. Of course, the tests must be carried out using results from *ab initio* calculations.

A test following the procedure of Sec. IV is easily carried out in the following way: The input data, namely, the three η_l at E_F and the four energy gaps discussed in Sec. III, are taken from a band calculation for a given potential, which we denote as V_A. The three logarithmic derivatives $\mathcal{L}_l^B(E)$, from a calculation for a quite different potential, V_B, are then taken as the reference logarithmic derivatives, $\mathcal{L}_l^{(0)}(E)$. The $\mathcal{L}_l(E)$ for A are then parametrized using Eqs. (2) and (4) and the seven pieces of data following steps (a)–(e) of Sec. IV.

In the remainder of this section we will discuss

the rather extensive tests that have been carried out using the procedure just outlined. The tests have been applied to the same four pairs of potentials for which the $v_l(E)$ are plotted in Figs. 1 and 2. More specifically, for Cu we have taken the $\mathfrak{L}_l^{(B)}$, the reference logarithmic derivatives, to correspond to the so-called l-dependent potential in one example and the Cu($\frac{2}{3}$) potential in the other. In both cases, the $\mathfrak{L}_l^A$ that we are attempting to parmetrize are those for the Chodorow potential. For Ag, the $\mathfrak{L}_l^B$ are for the so-called Ag(H) potential in one case and Ag($\frac{2}{3}$) potential in the other. In both Ag tests, the bands being parametrized are those for the Ag(HF) potential. It is to be emphasized that in all four cases the $E_n(\vec{k})$ corresponding to the reference logarithmic derivatives differ markedly from those being parametrized. This fact can be inferred from the $v_l(E)$ in Figs. 1 and 2. However, it is more clearly brought out in Fig. 3, in which the energy bands for the Ag($\frac{2}{3}$) and Ag(HF) potentials are plotted side by side for $\vec{k}$ along the ⟨100⟩ direction.

After parametrizing the $\mathfrak{L}_l^A$ for a given pair according to the prescribed method, we calculated the corresponding $E_n(\vec{k})$ for about 150 states along all of the symmetry axes and at the symmetry points. The resulting eigenvalues were then compared with those obtained directly using the known (original) logarithmic derivatives. All energies involved in the comparisons were computed in the same way with a maximum l of 2.

Some of the results of these comparisons appear in Table II, where the differences between the known band structures and the parametrized bands are given for the symmetry states at Γ, X, L, and W, from the lowest-energy levels, Γ_1 or X_1^l, up to relatively high energy for X_1^u. Note that all errors are given in units of 10^{-4} Ry. The errors for the X_5, X_3, and X_4, states, which are zero, are omitted since the energies are fitted there. Also tabulated for each test are the maximum deviation over the energy range from the lowest level up to the X_1^u level, which is 15 eV or larger, and the rms deviations for the approximately 150 states calculated for each band structure. The rms errors are gratifyingly small, being about 0.001 Ry. The larger errors, which in fact are not too large, occur at the extreme ends of the range, namely, at Γ_1 and X_1^u. For Γ_1 the errors result from the extrapolation of v_0 over the large range from E_F down to $E(\Gamma_1)$(~8 eV) and for X_1^u from the extrapolation of v_2 from E_F to $E(X_1^u)$ (~7 eV). The largest discrepancies are recorded for the case in which V_A and V_B correspond to Cu (Chodorow) and Cu($\frac{2}{3}$) potentials, respectively. This, we feel, is due to the relatively strong energy dependence of $v_2(E)$ and larger value of its slope at $E(L_1^u)$.[26]

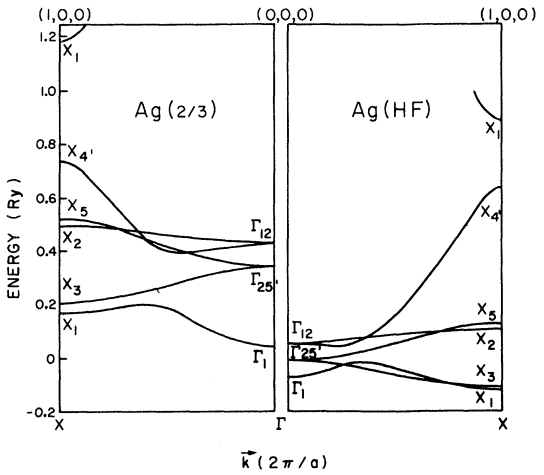

FIG. 3. $E_n(\vec{k})$ in the ⟨100⟩ direction for one of the four pairs of *ab initio* band structures used in the "realistic" test of Sec. V.

It is also noteworthy that the smallest errors occur in the case in which $\mathfrak{L}_l^A$ and $\mathfrak{L}_l^B$ are for the Ag(HF) and Ag($\frac{2}{3}$) potentials, respectively, for which the magnitudes of the v_l are in fact the largest. Clearly, the accuracy of the scheme depends on the nature of the energy dependences of the v_l rather than on their magnitudes. It is rather striking that the scheme could so closely reconcile two such disparate band structures as those shown in Fig. 3.

The results of these rather demanding tests are very encouraging. To put them in perspective we compare them with those obtained by a recent version of the combined tight-binding and nearly-free-electron scheme used by Smith and Mattheiss.[3] In that work, the 14 parameters employed were determined at energies which presumably were optimally distributed over essentially the whole energy range of interest (roughly the same as ours). Nevertheless, the accuracy[27] that they achieved compares unfavorably with that achieved by the present approach using half the number of the parameters in our demanding "realistic" tests.

Since comparisons of the previous GFM parametrization scheme with others were made in I, it is only necessary for us to compare the present results with those in I. The accuracy reported in I is definitely better in that the maximum error found over the same energy range was only 0.002 Ry. However, in the tests of I the coefficients were determined at a reasonably optimal set of energies. From our considerations of the sources of the large errors in the "realistic" tests above (the large extrapolations for v_0 and v_2), it is clear that the accuracy of the present scheme would ap-

TABLE II. Energy deviations (10^{-4} Ry) in the "realistic" tests for Cu and Ag. The logarithmic derivatives $\mathfrak{L}_l^A(E)$ and $\mathfrak{L}_l^B(E)$ associated with the indicated *ab initio* potentials are related by Eq. (2′). The manner in which they are used in the tests is described in Sec. V of the text.

$\mathfrak{L}^A$ / $\mathfrak{L}^B$	Cu Chodorow Cu l dependent	Cu Chodorow Cu ($\frac{2}{3}$)	Ag(HF) Ag(H)	Ag(HF) Ag($\frac{2}{3}$)
Γ_1	−9	120	85	1
$\Gamma_{25'}$	−11	−2	5	−12
Γ_{12}	−6	−6	4	−10
L_1^l	6	−2	14	−3
L_3	−11	−6	5	−12
L_3	−1	0	1	−3
$L_{2'}$	0	0	0	1
L_1^u	0	0	0	1
X_1^l	10	12	4	1
X_2	−2	−1	1	−3
X_1^u	82	156	27	3
$W_{2'}$	−3	−1	2	−6
W_3	−9	−5	4	−10
W_1^l	−6	−2	5	−9
$W_{1'}$	0	0	0	0
rms $\delta E_n(\vec{k})$	11	13	16	8
Maximum $\delta E_n(\vec{k})$	82	156	85	−18

proach that of I if a similarly optimal set of energies were used. Aside from the important fact that the present scheme requires fewer parameters, it has several other advantages, which will be mentioned in Sec. IX.

In an actual empirical application one would employ a reasonably good potential for which the associated band structure is fairly close to that required to fit experiments.[28] The resulting $v_l(E)$ should be smaller and smoother than those that we considered in the above examples. Thus we expect that a parametrization of a solid for which there are ample data would be at least as successful as those above.

VI. EMPIRICAL PARAMETRIZATION FOR CU AND AG

To proceed with the empirical parametrization, we must choose a set of reference $\mathfrak{L}_l^{(0)}(E)$ corresponding to a reference potential $V^{(0)}$. In Sec. V we demonstrated that the scheme accurately reproduced a first-principles band structure even when the logarithmic derivatives for a quite different band structure were used as the reference $\mathfrak{L}_l^{(0)}(E)$. Since the accuracy should be somewhat better if the reference $V^{(0)}$ and $\mathfrak{L}_l^{(0)}(E)$ differ only slightly from the corresponding "empirical" functions, we tried to select a reference potential whose band structure is in reasonable accord with experiment. For Cu we chose the Chodorow potential since its band structure has been shown to be in generally good accord with optical spectra and dimensions of the Fermi surface. For Ag, the reference potential was constructed from a superposition of atomic potentials and a local exchange correction with an adjustable coefficient α. From a preliminary investigation, we found by interpolation that a coefficient $\alpha = 0.778$ was a good choice.[29] The effective charge $2Z(r) = -rV(r)$ for the associated muffin-tin potential is tabulated in Table III.

We have already noted that Shaw *et al.*[8] were able to fit the Fermi-surface data for the noble metals for a wide range of E_F. We attempt to fit our larger set of data, which extend over an appreciable range of band energies, for this same range of E_F. Our purpose is to find out how sensitive the band structure is to changes in E_F.

The coefficients of $v_l(E)$ in Eq. (4) for Cu and Ag corresponding to the input data (Table I) are listed in Table IV for several E_F. The magnitudes of the v_l for a given E_F and the general E_F dependence of each coefficient are qualitatively similar

TABLE III. Effective charge, $2Z(r) = -rV(r)$, for the Ag ($\alpha = 0.778$) muffin-tin potential used as the reference potential in the empirical parametrization of Ag. The constant part of the potential is $V_C = -1.16305$ Ry and the inscribed sphere radius is $r_i = 2.7187$ a.u.

r	$2Z(r)$	r	$2Z(r)$	r	$2Z(r)$
0.01	89.501	0.46	25.224	1.38	6.375
0.02	85.338	0.50	23.386	1.42	6.100
0.03	81.591	0.54	21.737	1.46	5.846
0.04	78.186	0.58	20.253	1.50	5.611
0.05	75.073	0.62	18.914	1.58	5.191
0.06	72.206	0.66	17.697	1.66	4.831
0.07	69.542	0.70	16.583	1.74	4.522
0.08	67.051	0.74	15.554	1.82	4.257
0.09	64.714	0.78	14.600	1.90	4.030
0.10	62.515	0.82	13.712	1.98	3.837
0.12	58.484	0.86	12.887	2.06	3.674
0.14	54.867	0.90	12.121	2.14	3.539
0.16	51.599	0.94	11.409	2.22	3.429
0.18	48.635	0.98	10.750	2.30	3.342
0.20	45.939	1.02	10.140	2.38	3.277
0.22	43.476	1.06	9.576	2.46	3.234
0.24	41.214	1.10	9.055	2.54	3.210
0.26	39.133	1.14	8.575	2.62	3.207
0.28	37.215	1.18	8.131	2.70	3.224
0.30	35.447	1.22	7.722	2.78	3.260
0.34	32.309	1.26	7.344	2.86	3.316
0.38	29.620	1.30	6.995	2.94	3.393
0.42	27.284	1.34	6.673	3.02	3.489

for both metals. As the behavior is more satisfactorily exhibited graphically, we have plotted in Fig. 4 the $v_l(E)$ for Cu corresponding to two extreme values and the middle value of E_F. It can be seen that the v_l for Cu are not only larger for the extreme E_F but they (especially v_2) are more energy dependent.

To help study the relative band positions as a function of E_F, we have tabulated the energies of the symmetry states relative to E_F in Table V. It can be seen that for both metals the d bands move almost rigidly with changing E_F. The maximum change in relative position is less than 0.1 eV for the various E_F in the approximately 7-eV range. On the other hand, the other states which are not fixed by the data, e.g., the upper X, K, and W states, exhibit much larger variations with a change of E_F. The largest differences, about 2 eV, occur between the upper W_1 states for the two extreme E_F values. While some part of this variation could be attributable to errors in the scheme, we believe on the basis of the realistic tests that the major part of the changes truly reflects the dependence of the relative positions on E_F,[30] within the framework of the present scheme. It is thus possible that suitable experiments at sufficiently high energy and analysis of those experiments will lead to a considerable reduction in the range of possible E_F values. However, it appears that we cannot do so on the basis of the present data relating to band gaps.

Despite the above conclusion, there are certain considerations that are useful in limiting the possible E_F range. The values of E_F relative to V_c found in a large number of *a priori* calculations fall in the range 0.6 ± 0.1 Ry for Cu and 0.5 ± 0.1 Ry for Ag (both are roughly 0.7 in crystal units), values close to E_F for the free electron. This can be understood from the fact that d bands are at least 2 eV below E_F in the noble metals and that the positions of the s-p band levels relative to V_c (in contrast to those of the d bands) are not especially sensitive to changes in the potential for $r < r_i$. Clearly, the level structure for the extreme values of E_F corresponds to potentials which differ markedly from the usual *ab initio* potentials. The magnitudes of the differences in the potentials are roughly indicated by the magnitudes of the v_l, which are seen from Fig. 4 to be quite large for the extreme values of E_F. Thus, despite our inability to limit the E_F range empirically, we believe that the extreme E_F values which differ from the *a priori* values by 0.2 Ry or more are not physically acceptable. In Sec. VII, where comparisons with other calculations and experiments are made, we consider E_F values that lie in the physically plausible range.

TABLE IV. Coefficients entering Eq. (4) for the $v_l(E)$ for the empirical parametrization of Cu and Ag at several values of E_F. The $v_l(E)$, E_F, and energies in Eq. (4) are in crystal units.

	Cu					Ag				
E_F	0.9	0.8	0.690 398	0.45	0.3	0.9	0.8	0.75	0.5	0.35
S_0	−0.3675	−0.1898	−0.0152	0.2738	0.4227	−0.1884	0.0047	0.0896	0.4518	0.6267
S_1	0.1698	0.0861	−0.0038	−0.1175	−0.1738	0.3402	0.2517	0.2139	0.0723	0.0103
P_0	−0.4064	−0.1949	0.0025	0.3920	0.6034	−0.3280	0.0988	0.0986	0.4783	0.7269
P_1	0.0863	0.0223	−0.0265	−0.1312	−0.1901	0.2025	0.1383	0.1069	−0.0171	−0.0927
D_0	−0.4423	−0.2356	−0.0553	0.2174	0.3533	−0.0868	0.0329	0.0868	0.3190	0.4498
D_1	0.6231	0.3488	0.1085	−0.1213	−0.0793	0.1795	0.0565	0.0054	−0.1334	−0.1175
D_2	−0.4923	−0.3369	−0.1513	0.2251	0.4934	−0.4042	−0.3308	−0.2917	−0.1094	−0.0198

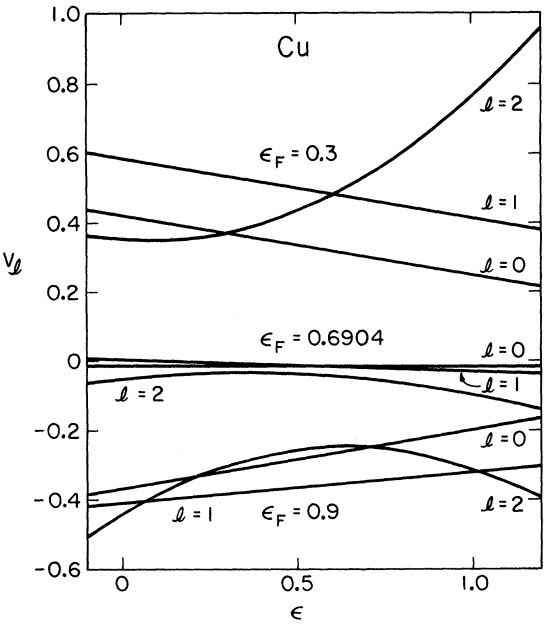

FIG. 4. Parametrized $v_l(E)$ for Cu with the reference logarithmic derivatives being those for the Chodorow potential. The functions are given for three values of E_F. The v_l, E, and E_F are in crystal units.

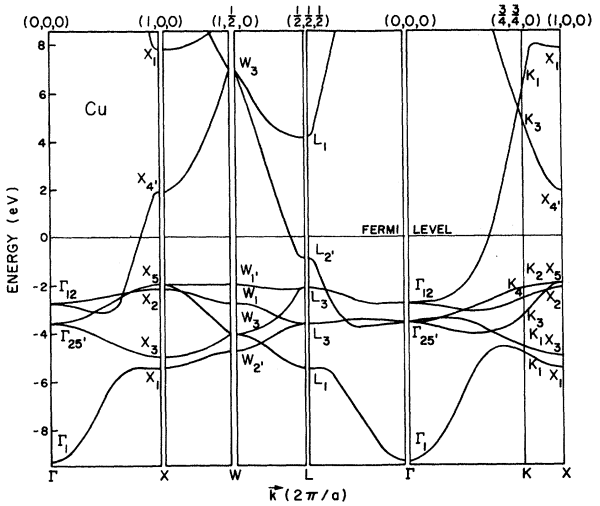

FIG. 5. Energy bands along the symmetry axes in the Brillouin zone corresponding to the empirically parametrized logarithmic derivatives for Cu for $E_F = 0.6904$ (crystal units).

VII. EMPIRICAL BAND STRUCTURES FOR CU AND AG: COMPARISONS WITH OTHER CALCULATIONS AND WITH EXPERIMENT

The purpose of this section is to compare the present results with those from several other calculations and with relevant experimental data. The empirical band structures that we will concentrate on are for the E_F values of 0.6904 crystal units (c.u.) for Cu and 0.750 c.u. for Ag, values near the middle of the ranges that we consider physically reasonable.[31] These $E(\vec{k})$ are exhibited in Figs. 5 and 6 for Cu and Ag, respectively, for $\vec{k}$ along all symmetry axes in the Brillouin zone. Before starting the comparisons we recall that these $E_n(\vec{k})$ have been required to precisely fit the input data in Table I. As a consequence, the Fermi-surface areas agree with the empirical values to within one part in 10^4 and the four key energy gaps agree with what we believe to be the most reliable values deduced from optical measurements.

A. Copper

Although it is generally useful to compare with previous calculations, this appears somewhat impractical in view of the rather large number of calculations for Cu and Ag that now exist. We will thus limit ourselves to comparisons with a small number of other investigations for each metal. We will relate the present bands for Cu to the results of Janak *et al.*[32] and to the $E_n(\vec{k})$ for the Chodorow potential, since these bands have received considerable attention and have been used in a number of other studies. For this purpose, a number of representative energy gaps are listed in Table VI. From the tabulation it can be seen that the d bands for the Chodorow and present band structures are virtually the same. Roughly speaking, the conduction-band symmetry states (e.g., Γ_1, $L_{2'}$, L_1^u, and X_1^u) of our empirical $E_n(\vec{k})$ tend to be separated further from the

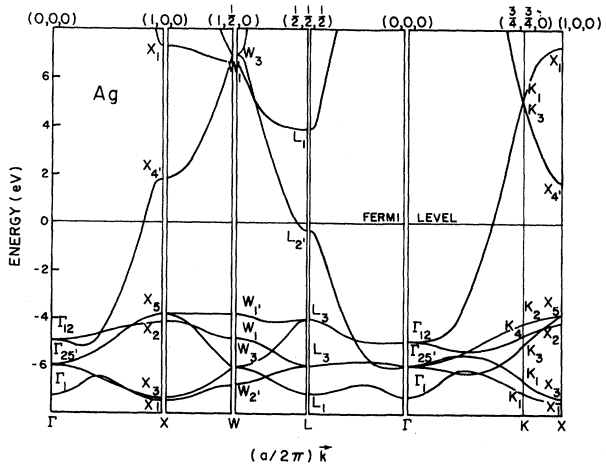

FIG. 6. Energy bands along the symmetry axes in the Brillouin zone corresponding to the empirically parametrized logarithmic derivatives for Ag for $E_F = 0.75$ (crystal units).

TABLE V. Energies (in eV) of symmetry states of Cu and Ag relative to the Fermi level obtained from the empirical parametrization scheme for several values of E_F (in crystal units).

	Cu			Ag		
E_F	0.9	0.6904	0.3	0.9	0.75	0.35
Γ_1	−9.00	−9.31	−9.26	−7.20	−7.30	−7.21
$\Gamma_{25'}$	−3.64	−3.59	−3.50	−5.96	−5.94	−5.87
Γ_{12}	−2.80	−2.77	−2.70	−4.96	−4.95	−4.87
X_1	−5.52	−5.46	−5.33	−7.49	−7.43	−7.34
X_3	−4.96	−4.96	−4.96	−7.31	−7.31	−7.31
X_2	−2.17	−2.17	−2.15	−4.14	−4.13	−4.10
X_5	−1.96	−1.96	−1.96	−3.81	−3.81	−3.81
$X_{4'}$	1.90	1.90	1.90	1.84	1.84	1.84
X_1	8.13	7.81	7.34	7.19	7.29	7.33
L_1	−5.42	−5.45	−5.47	−7.15	−7.17	−7.16
L_3	−3.70	−3.65	−3.54	−6.15	−5.99	−5.90
L_3	−2.14	−2.13	−2.11	−4.08	−4.07	−4.04
$L_{2'}$	−0.92	−0.90	−0.86	−0.36	−0.35	−0.33
L_1	4.12	4.14	4.18	3.87	3.88	3.90
K_1	−4.94	−4.90	−4.82	−7.08	−7.04	−6.96
K_1	−4.44	−4.57	−4.34	−6.60	−6.59	−6.54
K_3	−3.21	−3.21	−3.17	−5.06	−5.06	−5.04
K_4	−2.65	−2.61	−2.53	−4.71	−4.67	−4.61
K_2	−2.18	−2.17	−2.14	−4.13	−4.12	−4.08
K_3	5.20	4.89	4.64	5.27	4.94	4.57
K_1	6.22	6.34	6.13	5.02	5.45	5.99
$W_{2'}$	−4.81	−4.73	−4.57	−6.80	−6.76	−6.65
W_3	−4.03	−4.01	−3.97	−6.07	−6.07	−6.04
W_1	−2.84	−2.78	−2.67	−4.92	−4.87	−4.78
$W_{1'}$	−1.96	−1.96	−1.96	−3.81	−3.81	−3.81
W_3	7.47	6.96	6.51	7.30	6.89	6.46
W_1	8.00	9.30	10.38	6.03	6.65	8.14

Fermi level than are those for the Chodorow bands. Our Γ_1 level is lower relative to d bands by about 0.02 Ry. It is to be noted that the position of the Γ_1 level cannot be determined by available data, but many of the other levels considered can be and are thus more critical. The Chodorow $L_{2'}$ and $X_{4'}$ levels are higher relative to the d bands by about 0.02 and 0.01 Ry, respectively. On the other hand, the upper L_1 and X_1 level are relatively lower for the Chodorow bands than for the present bands by 0.015 and 0.04 Ry, respectively. The significance of these differences will be evident when we compare the present results to experiment.

In connection with the above comparisons we note that Williams *et al.*[33] in their calculations of $\epsilon_2(\omega)$ have used the Chodorow phase shifts, except that they modified the η_2 around $E(L_1^u)$ so as to raise the L_1^u level by 0.3 eV. The L_1^u level is higher in the present bands than in the Chodorow bands by 0.2 eV; the $L_1^u - L_{2'}$ gap has been widened further by a 0.3-eV lowering of $L_{2'}$. From these observations it appears that the $E_n(\vec{k})$ obtained by Williams *et al.* lie between the Chodorow and the present $E_n(\vec{k})$.

Next we compare with some of the results of Janak *et al.*,[32] who carried out self-consistent calculations using several local exchange-correlation potentials. The energy separations listed in Table VI are those for the local exchange-correlation potential with the α coefficient ($\alpha = 0.77$) which gave the closest agreement with Fermi-surface data. The discrepancies between these gaps and those for the present band structure are relatively small, the largest being 0.019 Ry for the $L_1^u - L_{2'}$ separation with oug gaps being larger in all cases. Further, if one considers the energy levels relative to E_F one finds that the differences between the two calculations tend to grow roughly linearly with $E - E_F$. This relationship seems to correlate with the results of the Sham-Kohn[34] theory of elementary excitations of an electron gas. In that theory it is found that for low excitation energies $[E(\vec{k}) - E_F \ll E_F]$ the effective one-electron interaction is given by

$$V(E, \vec{r}) = V(\vec{r}) + (E - E_F)[1 - m^*(n(\vec{r}))] + O((E - E_F)^2) \tag{11}$$

TABLE VI. Comparison of energy gaps (in Ry) for the present energy bands with those from other calculations.

	$X_5 - \Gamma_1$	$X_5 - X_1^l$	$X_{4'} - X_5$	$X_1^u - X_5$	$E_F - L_3^u$	$E_F - L_{2'}$	$L_1^u - L_{2'}$	$L_3^u - L_3^l$	$W_1^u - W_{1'}$
Cu									
Chodorow potential (Refs. 13, 14)	0.517	0.249	0.302	0.695	0.154	0.045	0.341	0.104	0.820
Janak *et al.* (Ref. 32)	0.525	0.242	0.270	...	...	0.061	0.351	...	...
Present work	0.541	0.257	0.284	0.719	0.157	0.066	0.370	0.111	0.828
Ag									
CKS (Ref. 4)	0.305	0.290	0.398	0.769	0.292	0.022	0.314	0.142	0.898
Christensen (Ref. 40)	0.266	0.239	0.434	0.759	0.300	0.011	0.256	0.289	0.801
Present work	0.256	0.268	0.415	0.818	0.299	0.026	0.311	0.141	0.771

and, correspondingly, the excitation energies are

$$E(\vec{k}) - E_F = \frac{\epsilon(\vec{k}) - E_F}{\langle m^*(n)\rangle_{\vec{k}}}, \tag{12}$$

where the $V(\vec{r})$ is the energy-independent potential appropriate to the ground state in the local approximation, the $\epsilon(\vec{k})$ are the eigenvalues for this potential, and $m^*(n(\vec{r}))$ is the density-of-states effective mass for electron density $n(\vec{r})$. The relationship between our excitation energies and the relative energies of Janak *et al.* parallels that of Eq. (12), with their energies appropriately playing the role of the $\epsilon(\vec{k}) - E_F$. A similar correlation has been pointed out for β-brass and for Cu by Moruzzi *et al.*[35] Their results indicate a value of 1.08 for the $(m^*)^{-1}$ factor, which is close to but slightly larger than our estimate of 1.05. It should be noted that, while Eq. (11) is the result of a low-excitation expansion, several of the levels considered above correspond to moderately large excitations. Also worth noting is the fact that the effective interaction in Eq. (11) is a local l-independent operator, whereas the empirical interactions are found to be l dependent.

Since the question raised in Sec. II about the possibility of $\mathfrak{L}_l(E)$ being monotonic is related to the E dependence of the effective potential [see Eq. (3)], it is useful to consider that question here. From Eq. (11) it is seen that $\partial V/\partial E \approx 1 - m^*$, which is a small fraction of unity. Thus for low excitation energies $d\mathfrak{L}_l/dE < 0$, just as in the case of an E-independent potential. Furthermore, the comparison of the empirical bands with those of Janak *et al.* indicates that this result should apply for the larger range of E that we have been considering. The monotonicity of $\mathfrak{L}_l$ in addition to $\mathfrak{L}_l^{(0)}$ in turn implies that $E + v_l(E)$ is a monotonically increasing function of E.

We now consider how the empirical Cu band structure agrees with data that were not used in the parametrization. Much of the information that will be employed in the comparison has come from a detailed (II) analysis of Gerhardt's[21] piezo-optical response functions for Cu. Similarly, the results of an analysis of Nilsson and Sandell's[22] response functions for Ag will be used in the following subsection.

First we note that one of the energy gaps which is most accurately determined from the piezo-optical data is the threshold for the interconduction band transitions around L, i.e., $Q_-(E_F) \rightarrow Q_+(L_1^u)$. This value is 4.23 ± 0.05 eV. For our empirical bands the value is 4.21 eV, which is in very good accord with experiment. The value for the Chodorow bands is 3.9 eV.[36]

In regard to the details of the $d(\text{top}) \rightarrow E_F$ transitions, we recall (Sec. III) that we have taken the 2.10-eV threshold energy to correspond to the $\Delta_5 \rightarrow \Delta_1(E_F)$ transition. The calculated value for the threshold in the vicinity of L, $Q_+(L_3^u) \rightarrow Q_-(E_F)$, is 2.14 eV. Probably the best experimental value for this threshold is derived from the 2.20-eV peak in the isotropic piezo-optical response function,[21] $W_{11} + 2W_{12}$. When the appropriate shift due to broadening ($\Gamma/\sqrt{3}$) is subtracted out ($\Gamma \approx 0.10$ eV), the threshold value of 2.14 ± 0.05 eV is obtained, which coincides with the calculated value.

The $Q_-(L_3^u)$ band also contributes to the optical properties with a threshold $Q_-(L_3^u) \rightarrow Q_-(E_F)$ which the calculation predicts to be 2.71 eV. This contribution, which is masked by other contributions in $\epsilon_2(\omega)$, produces a discernible structure in both the trigonal (W_{44}) and tetragonal ($W_{11} - W_{12}$) response functions at 2.6–2.8 eV.

Other unambiguous structures in the Cu piezo-optical data are the large shoulder at approximately $\hbar\omega = 4.7$ eV in $W_{11} + 2W_{12}$ and the positive peak in $W_{11} - W_{12}$ at 4.1 eV. The former we attribute to transitions starting with the lowest Σ_1 band to the $\Sigma_1(E_F)$, for which the calculations predicts a 4.71-eV threshold. The latter we assign to the $\Sigma_1(\text{third band}) \rightarrow \Sigma_1(E_F)$ and $\Sigma_3 \rightarrow \Sigma_1(E_F)$ transitions, which the calculations show are nearly degenerate and start at 3.97 and 3.99 eV, respectively.

Analysis of the photoemission associated with the interconduction band transitions have been made which yield the value of $E_F - L_{2'}$. Lindau and Wallden,[37] using a two-band model have obtained the value $E_F - L_{2'} = 0.75$ eV from their data. However, we have also analyzed their photemission data using a two-band model in which the effects of broadening are fully incorporated and were able to obtain good agreement with our 0.90-eV value. Smith,[38] using a two-OPW model and a $L_1^u - L_{2'}$ gap of 4.2 eV, concluded that the $E_F - L_{2'}$ difference is 0.7 eV. With the correct gap of 5.04 eV his model would yield a $E_F - L_{2'}$ separation slightly greater than 1 eV. But we believe that a more quantitative treatment, including broadening, would lead to a value very close to our 0.90 eV. At this point it should be noted that to a large extent the position of $L_{2'}$ relative to E_F is fixed by the interconduction band threshold $[Q_+(k_F) - E_F]$ and gap $(L_1^u - L_{2'})$, both of which are known accurately. It is also fixed by the area of the Fermi-surface neck. In a related fashion, the $E_F - L_{2'}$ gap for the Chodorow bands[13,14] is small (0.6 eV) and the neck area is too low by about 30%.[33]

The other optical gap that we can compare with is the 5.32-eV $Q_+(L_1^l) \rightarrow Q_-(E_F)$ transition identified by Pells and Shiga.[39] The value for the present

bands is 5.29 eV. Unless the identification is incorrect, this agreement indicates that even the lower d levels, for which the input data are least precise, are given accurately.

Since we have not as yet calculated $\epsilon_2(\omega)$, a direct comparison with this function is not presently possible. However, in view of the very good agreement of the empirical bands with the large amount of information about energy separations, we expect the present bands to yield a dielectric constant in good agreement with experiment. In this connection, we recall the apparent near-agreement of our results with the bands of Williams *et al.*,[33] which in turn yielded an $\epsilon_2(\omega)$ in good accord with experiment. As these authors noted, the interband transitions around L are quite important in these calculations. The threshold for the present bands, 4.2 eV, is the same as their value, while our 5.04-eV $L_1^u - L_{2'}$ gap is slightly larger than their 4.9-eV value. In regard to detail, it appears that the small shift of the peak to higher energies would in fact improve the agreement with experiment.

B. Silver

For this metal we compare our results with the semiempirical bands obtained by CKS and the most recent calculation by Christensen.[40] The comparison is made in the last three lines of Table VI. The results of CKS are considered first. We note that the agreement between these bands and the present ones is quite close from the d-band region up to $E(L_1^u)$. This, of course, follows from the fact that almost the same set of empirical data was used in both calculations. The structure of the d band is almost identical in both cases. The only difference is that the deepest d-band states are somewhat lower in CKS, due to the fact that the $L_3^u - X_3$ gap was set equal to 3.5 eV (the measured d-band width) in CKS, while $X_5 - X_3$ is given that value here. One other difference for energies below E_F is that the CKS Γ_1 value (which was taken from a previous calculation) is relatively lower than that in the present results by 0.05 Ry. It can also be seen that at energies at and above $E(X_1^u)$ there are significant discrepancies and that these increase with E. Although these high energies were outside the range of primary interest in CKS, it is worthwhile to consider them and thus the different manners in which the two schemes extrapolate. It was noted in CKS that the functional forms used to fit the $\tan\eta_l$ did lead at high E to significant differences from the quantities obtained in the *ab initio* calculations. In contrast, it was shown by the realistic tests of Sec. V that the present approach does not lead to large errors in this range. The reason for this is that in the present scheme we are extrapolating only the correction term, the $v_l(E)$ in $\mathfrak{L}_l^{(0)}(E + v_l(E))$, but not the primary quantity, the $\mathfrak{L}_l(E)$ or $\tan\eta_l(E)$.

In the recent work that we are concerned with here, Christensen[40] calculated the relativistic energy bands of Ag. Since our results were obtained from the nonrelativistic form of the GFM, the validity of a comparison with Christensen's results might be questioned. We believe that since empirical data have been used to determine the $\mathfrak{L}_l(E)$ all relativistic effects except the spin-orbit splittings are largely included in our results. Thus, to carry out the comparison we have, where necessary, appropriately averaged[41] Christensen's energies for the components of the spin-orbit split levels. The comparison shows that for energies below E_F the differences between Christensen's and the present results are not too large, although they are generally larger than between the CKS and present bands. The largest discrepancy here concerns the d-band width with Christensen's being narrower than ours by approximately 0.4 eV. Also, his p-like levels appear to be slightly higher than ours, leading to $E_F - L_{2'}$ and $X_{4'} - X_5$ separations which are roughly 0.2 eV lower and higher, respectively, than those for the present bands, which closely agree with experiment. As is evident from Table VI, however, the most serious discrepancies occur for the higher-energy levels, e.g., the L_1^u and X_1^u. Christensen's $L_1^u - L_{2'}$ and $\chi_1^u - \chi_5$ gaps are roughly 0.75 and 0.8 eV smaller than the corresponding present gaps. In terms of confronting experiment, the gap at L is the relevant one. Christensen has argued, with some reservation, that his 3.5-eV value and not the 4.2 eV value that we employ here correctly represents the optical transition energy for $L_{2'} \to L_1^u$. We believe that the direct optical and photoemission studies firmly support the more commonly accepted identification which is used in this work. However, we believe that the most unambiguous evidence for this conclusion is contained in the piezo-optical response functions. It will be shown in II that the detailed shapes and magnitudes of the relevant parts of the $W_{ij}(\omega)$ tensor for $\hbar\omega \simeq 3.9$–4.4 eV are in accord with the $L_{2'} \to L_1^u$ identification. Consequently, we feel that the present bands much more accurately represent the band structure for the energies involved.

There are considerably fewer extra experimental data available for checking the empirical Ag bands than there were for Cu. As in the case of Cu, the prominent structure in the trigonal response function corresponding to the interconduction band transitions allows for an accurate determination of the threshold energy as well as the gap at the critical point L. From the analysis of

II, the threshold for $Q_-(E_F) \rightarrow Q_+(L_1^u)$ is 3.87 ± 0.05 eV. The calculated value is 3.90 eV.

Photoemission studies and analysis by Smith[38] have yielded a value of 0.3 eV for the $E_F - L_{2'}$ gap, while Wallden and Gustafson[42] obtained the value 0.31 eV. The $E_F - L_{2'}$ difference for the empirical bands is 0.35 eV, which is quite consistent with the above values. As pointed out in the discussion for Cu, this energy difference is largely fixed by the values for the interconduction band threshold and critical-point gap at L. The consistency of these two independent measurements thus further confirms our interpretation as opposed to that of Christensen.

Christensen's value for the separation of $L_{2'}$ from E_F is roughly half our value. It follows that the cross-sectional area of the necks of the Fermi surface for his bands will only be about half the measured value. Also, as Christensen noted, his values for the Fermi-surface belly radii differ from the experimental values by a few percent. The errors for present bands are about 0.1 of 1%[8].

The only other datum for Ag is the weak structure appearing at about 9.3–9.7 eV in the $\epsilon_2(\omega)$, reported by Ehrenreich and Philipp,[24] which they assigned to the $X_1^l \rightarrow X_{4'}$ transition. The calculated energy for this transition is 9.25 eV. However, we note that the transitions with the threshold at $\Delta_1(X_{4'}) \rightarrow \Delta_1(X_1^u)$ also start at approximately 9.3 eV. It turns out that the square of the matrix elements[43] for the $X_{4'} \rightarrow X_1^u$ transition is larger by a factor of nearly 20 than that for $X_1^l \rightarrow X_{4'}$. Thus even with a smaller density-of-states factor, this implies that the $\Delta_1 \rightarrow \Delta_1$ transitions would probably dominate and be responsible for the structure. We note, however, that some caution should be exercised in the use and interpretation of data at such high energies.

In concluding this discussion, we remark that, although the present Ag band structure agrees with available data, it has not been checked as extensively as the band structure of Cu because of the more limited data. We expect that additional data relating to the interband transitions above 5 eV or so would be very helpful in providing the desired additional checks. We feel that piezo-optical measurements in single crystals would be particularly useful in this energy range. For example, a structure associated with the $X_5 \rightarrow X_{4'}$ transition (with the X_5 split by spin-orbit coupling) should appear in the tetragonal response functions and be amenable to detailed analysis.

VIII. RELATION OF v_l TO EFFECTIVE POTENTIAL

In addition to developing a means for accurately obtaining electronic structure, an empirical scheme could in principle provide some information about the effective one-body interaction which includes via the self-energy correction many-body contributions. The electronic structure deduced from empirical data has these contributions built into it. As noted earlier, an important virtue of GFM scheme over other approaches is that the quantities that are determined in an empirical application, namely, the $\mathcal{L}_l(E)$, have a clear physical interpretation. They are directly related to the effective potential, $V_l(E,r)$, through the one-body Schrödinger equation. In this section we discuss this relationship.

To proceed we consider the equation for the radial function $P_l^{(0)}(E,r) = rR_l^{(0)}(E,r)$ associated with the reference potential $V^{(0)}(r)$,

$$\left(-\frac{d^2}{dr^2} + \frac{l(l+1)}{r^2} + V^{(0)}(r)\right) P_l^{(0)}(E_0,r) = E_0 P_l^{(0)}(E_0,r), \tag{13}$$

and the equation for radial function $P_l(E,r)$ for $V_l(E,r)$,

$$\left(-\frac{d^2}{dr^2} + \frac{l(l+1)}{r^2} + V_l(E,r)\right) P_l(E,r) = E P_l(E,r). \tag{14}$$

By multiplying Eq. (14) by $P_l^{(0)}(E_0,r)$ and Eq. (13) by $P_l(E,r)$, subtracting, and then integrating from $r=0$ to $r=r_i$, one obtains the following relation for the logarithmic derivatives:

$$\begin{aligned}[\mathcal{L}_l(E) - \mathcal{L}_l^{(0)}(E_0)] P_l(E,r_i) P_l^{(0)}(E_0,r_i) &= (E-E_0)\int_0^{r_i} P_l(E,r) P_l^{(0)}(E_0,r)\,dr \\ &\quad - \int_0^{r_i} \delta V_l(E,r) P_l(E,r) P_l^{(0)}(E_0,r)\,dr,\end{aligned} \tag{15}$$

where

$$\delta V_l(E,r) \equiv V_l(E,r) - V_0(r). \tag{16}$$

This relationship itself is useful, and it simplifies for $E = E_0$. But it can be made even more useful for our particular parametrization scheme by utilizing our *Ansatz* [i.e., Eq. (2)] for $\mathcal{L}_l(E)$ and taking $E_0 = E + v_l(E)$. This results in the relatively simple relationship

$$v_l(E) = -\frac{\int_0^{r_i} P_l(E,r)\,\delta V_l(E,r)\,P_l^{(0)}(E+v_l(E),r)\,dr}{\int_0^{r_i} P_l(E,r)\,P_l^{(0)}(E+v_l(E),r)\,dr}. \tag{17}$$

Since the $v_l(E)$ are determined over a certain energy range by the parametrization, Eq. (17) provides information about $V_l(E,r)$ over that range. However, Eqs. (14) and (17) constitute a quite complex set of coupled nonlinear equations. For the case of small δV_l these equations are approxi-

mately linear.

One solution to Eqs. (14) and (17) is known, namely, $\delta V_l(E,r) = -v_l(E)$ and $P_l(E,r) = P_l^{(0)}(E + v_l(E), r)$, as can be easily demonstrated. That this should be a solution is not surprising, since the square-well correction potentials were the ones that motivated the present parametrization scheme. However, it is important to note that this is not a unique solution. It is clear physically that there should be r-dependent solutions. In fact, for a given E Eq. (17) merely fixes a quantity similar to an expectation value of $\delta V_l(E,r)$. It appears that only when considerable restrictions are imposed on the form of δV_l will the equations yield a unique solution. It may be of interest to note that the problem of determining δV_l is closely related to the "inverse"-scattering problem.

Despite the nonuniqueness problem, the above equations should be useful in that they provide a direct connection between the desired functions, δV_l and P_l, and the parametrized $v_l(E)$. It is reasonable to expect that the $\delta V_l(E,r)$ will be fairly smooth functions of E and r, and further that many-body theory will provide some guidance for their functional forms. An example of this is given by Eq. (11), which is a result of the Sham-Kohn[34] theory. When suitably parametrized functional forms for the $\delta V_l(E,r)$ are obtained, the equations will provide the means for determining the parameters.

As a very simple example of the above procedure we have taken the potential correction to have the form

$$\delta V_l(E,r) = a_l(E)r + b_l(E)r^2$$

and have required in one case that they have vanishing slope at $r = r_i$ and in another that they vanish at $r = r_i$. Equations (14) and (17) were then solved self-consistently for the one independent function, the $a_l(E)$, say, and for the radial functions using the empirical $v_l(E)$ for Cu and $E_F = 0.6904$. The calculations converged in two or three iterations starting with $P_l = P_l^{(0)}(E + v_l(E), r)$. We find that the energy dependences of the $a_l(E)$ [and thus the $b_l(E)$] roughly parallel those of $-v_l(E)$. This is not surprising since the δV_l do not change sign.

One important practical reason for seeking an empirically corrected potential is to enable one to obtain "corrected" wave functions which are needed for the calculation of matrix elements. Even before we can resolve the nonuniqueness problem, approximate wave functions can be obtained from the present scheme. The crudest approximation would be to use the radial functions $R_l^{(0)}(E,r)$ for the reference potential. A better approximation is $R_l^{(0)}(E + v_l(E), r)$, which we believe incorporates the effects of δV_l in a reasonable way, even when the δV_l does not have the square-well form. We speculate that for $v_l(E)$ that are not large these functions and the matrix elements that result from them would differ only slightly from those corresponding to other forms of δV_l, providing that the δV_l satisfy some smoothness criterion.[44] We plan to check this speculation shortly. We note that a criticism which has been raised against the use of empirical band approaches like the present one is that they fail to provide a means for obtaining wave functions. From the above discussion it is seen that the present scheme does not suffer from that shortcoming.

IX. SUMMARY AND DISCUSSION

The present work has accomplished what we believe to be the most satisfactory empirical parametrization of the electronic structure of a d-band metal over a broad energy range. Further, the results for the specific metals studied, namely, Cu and Ag, appear to be in good agreement with all available information. The success of this work is mainly attributable to the development of a new parametrization scheme. In this new approach the logarithmic derivative, $\mathfrak{L}_l(E)$, for a given l is represented by the corresponding quantity obtained in an *ab initio* calculation, but with the energy shifted by a quantity $v_l(E)$, which could be viewed as the depth of an l- and E-dependent square-well potential. These $v_l(E)$ for $l = 0$, 1, and 2 were shown to be very smooth functions of E which could be accurately parametrized over the energy range of interest (roughly 1 Ry) with only seven adjustable parameters for a d-band metal—a number which is quite reasonable for a fully empirical application in view of the data presently available.

Many of the advantages of the present scheme over the previous GFM and the other parametrization approaches can be understood in terms of the nature of the $v_l(E)$ and $\mathfrak{L}_l^{(0)}(E)$. The smoothness of the $v_l(E)$, which is reflected in the ease with which they can be parametrized with low-order polynomials, has several consequences: (i) It enables us to circumvent the difficulty previously encountered in fitting the singular $\mathfrak{L}_2(E)$ or $\tan\eta_2(E)$; (ii) the number of adjustable parameters required for accurate results is very small (smaller than that needed in any previous scheme); (iii) the accuracy is less sensitive to the energies at which the parameters are determined.

In connection with points (ii) and (iii) above, we note that realistic tests of the accuracy of the present scheme were conducted in precisely the same manner as proposed for the fully empirical parametrization (Sec. V). The $E_n(\vec{k})$ for some *ab initio* calculations were parametrized using as the

reference logarithmic derivatives, $\mathfrak{L}_l^{(0)}(E)$, those corresponding to a quite different band structure (e.g., see Fig. 3). The accuracy achieved in our test for four different pairs of band structures (typical rms and maximum errors were 0.001 and 0.01 Ry, respectively) is higher than that achieved in the other schemes in less demanding tests using more parameters.

From the role played by the reference $\mathfrak{L}_l^{(0)}(E)$, it is evident that this approach can be used naturally and conveniently to blend empirical data into a first-principles calculation. Related to this point is the flexibility of the scheme regarding the number of adjustable parameters to be used. The number can readily be varied depending on the data available and the accuracy required. If, for example, only a few pieces of data are available, one could use only the constant terms in Eq. (4) for the $v_l(E)$, which corresponds to a rigid shifting of the $\mathfrak{L}_l^{(0)}(E)$ curves. This should provide a substantial correction to the bands over a reasonable range of E. There is also flexibility in the maximum value of l to be used. For reasonably high energies [e.g., $E \gtrsim E(L_1^u)$] the inclusion of the $l = 3$ component produces noticeable energy shifts. However, since the $\tan\eta_3$ are still relatively small, the use of the unmodified $\mathfrak{L}_3^{(0)}(E)$ should suffice, with the consequence that no new parameters need be introduced. Still another advantage is that the present approach extrapolates to relatively high energy better than schemes in which the $\mathfrak{L}_l(E)$ [or $\tan\eta_l(E)$] are themselves represented by some functional form.

In the present work we have concentrated on the electronic structure of d-band metals, but clearly the general approach can be applied to other types of solids. The result of a test carried out on Al indicates that the approach would be useful for simple metals. For Al four or at most five parameters should suffice for accurate results over a large energy range. From experience we are confident that the approach will be useful for any solid for which the muffin-tin potential is a useful approximation.

It has been emphasized that the GFM parametrization scheme, in contrast to many other approaches, could provide an effective means for obtaining useful information about the effective potential $V_l(E, r)$ and the associated wave functions. Progress in this connection has been realized by the derivation of coupled equations connecting these quantities with the parametrized $v_l(E)$. One solution to these equations for energy E consists of the potential $V_l(E, r) = V^{(0)}(r) - v_l(E)$ and the radial function $R_l^{(0)}(E + v_l(E), r)$. However, it is clear that Eqs. (14) and (17) do not admit unique solutions unless sufficient constraints are imposed on potential corrections $V_l(E, r) - V^{(0)}(r)$. Nevertheless, we suggest that $R_l^{(0)}(E + v_l(E), r)$ provides a reasonable good approximation for practical applications. To the extent that this is true, we have eliminated the objection raised against empirical band schemes that they fail to provide wave functions.

Because of the important role of experimental data in the present work, careful consideration was given to their selection. The seven pieces of data for each metal consisted of the three phase shifts at E_F accurately determined by the Fermi-surface dimensions and the energies of four optical gaps for transitions whose identifications we believe are firmly established. The gaps locate four levels (X_5, $X_{4'}$, X_3, and L_1^u) relative to E_F at energies ranging from the bottom of the d band (~5 and 7.5 eV below E_F for Cu and Ag) to $E(L_1^u)$ (~4 eV above E_F for both). The empirical bands are thus required to be "correct" at key energies over this appreciable and important (empirical) range. Thus on the basis of the realistic tests we have strong expectations that the empirical bands will also be correct for other energies within the empirical range, and also for energies somewhat outside the range. The fact that these empirical band structures agree with all additional information available about level positions tends to confirm our belief. Since there is a significant amount of additional data for Cu, we believe that the empirical Cu bands have been checked in considerable detail. The situation is somewhat different for Ag, where the additional data are quite limited due to the fact that much of the relevant interband structure occurs for $\hbar\omega \gtrsim 5.5$ eV, where the data are rather sparse. Additional optical data, especially piezo-optical measurements on single crystals, would be very useful in further checking the Ag empirical band structure.

As is well known, the Fermi-surface data[8,45] can be parametrized over a wide range of E_F. We have parametrized the band structures over the same E_F range. Our results indicate that the relative positions of levels lying in the energy range covered by the input data are rather fixed, while the higher-energy states are relatively sensitive to E_F. As a consequence, it does not appear possible to limit the possible E_F range using the present data, but it should be possible if some high-energy transitions (in the 10-eV range) can be firmly identified. Further, we argue that plausible physical considerations can be used to narrow the E_F range.

There are a few aspects of our work on the noble-metal energy bands that remain to be done. One is the extension to the relativistic problem. The present approach should still be useful, al-

though a larger number of parameters will probably be needed. The relativistic formulation is a necessity for treating Au; it would also be desirable for Ag. Also, we have not as yet carried out calculations of the imaginary part of the dielectric function. The $\epsilon_2(\omega)$ calculation and the extension to relativistic bands will be the subject of future work.

In conclusion, we remark that the success of the present scheme is due to its exploitation of the information contained in *ab initio* logarithmic derivatives. Although initially it sounds contradictory, it is this exploitation of the first-principles results which enables us to undertake what we loosely term our "fully empirical"[9] parametrization of Cu and Ag.

ACKNOWLEDGMENTS

We are grateful to Dr. G. P. Pells for sending us the $\epsilon_2(\omega)$ data for Cu and his unpublished data for Ag, to Dr. J. T. Waber for supplying us with atomic charge densities for Cu and Ag, and to Dr. A. R. Williams, Dr. J. F. Janak, and Dr. V. L. Moruzzi for sending us the dipole-matrix elements for Cu.

---

†Work supported by the National Science Foundation.

*Present address: Dept. of Physics, Auburn University, Auburn, Ala. 36830.

[1]H. Ehrenreich and L. Hodges, in *Method in Computational Physics, Energy Bands of Solids*, edited by B. Alder, S. Fernbach, and M. Rotenberg (Academic, New York, 1968), Vol. 8, Chap. 5; J. C. Phillips and R. Sandrock, *ibid.*, Chap. 2; F. M. Mueller, Phys. Rev. 153, 659 (1967).

[2]C. Y. Fong and M. L. Cohen, Phys. Rev. Lett. 24, 306 (1970).

[3]N. V. Smith and L. F. Mattheiss, Phys. Rev. B 9, 1341 (1974).

[4]B. R. Cooper, E. L. Kreiger, and B. Segall, Phys. Rev. B 4, 1734 (1971) (referred to as CKS throughout).

[5]A.-B. Chen, B. Segall, B. R. Cooper, and E. L. Kreiger, Phys. Rev. B 9, 3207 (1974) (referred to as I throughout). References to other parametrization schemes are cited here.

[6]B. Segall and F. S. Ham, in *Method in Computational Physics, Energy Bands of Solids*, edited by A. Alder, S. Fernberg, and M. Rotenberg (Academic, New York, 1968), Vol. 8, Chap. 7.

[7]J. Korringa, Physica XIII, 392 (1947); W. Kohn and N. Rostoker, Phys. Rev. 94, 1111 (1954).

[8]J. C. Shaw, J. B. Ketterson, and L. R. Windmiller, Phys. Rev. B 5, 3894 (1972).

[9]By a "fully empirical" parametrization we mean one in which values of the parametrized quantities, the $v_l(E)$ [see Eqs. (2) and (4)], are determined wholly by experimental data throughout the energy range of interest. In a strict sense, the final $\mathfrak{L}_l(E)$ do depend on the first-principles $\mathfrak{L}_l^{(0)}(E)$ that are employed in the parametrization. However, as the results of this work indicate, the final $\mathfrak{L}_l(E)$ are in a practical sense rather independent of the choice of any "reasonable" set of $\mathfrak{L}_l^{(0)}(E)$.

[10]We want to limit the maximum error in the $E_n(\vec{k})$ to about 0.1 eV.

[11]A. Messiah, in *Quantum Mechanics* (North-Holland, Amsterdam, 1964), Vol. 1, Eq. (III.28).

[12]The *ab initio* potential can be E dependent. The requirement is only that the right-hand side of Eq. (3) must be less than zero.

[13]B. Segall, Phys. Rev. 125, 109 (1962).

[14]G. A. Burdick, Phys. Rev. 129, 138 (1963).

[15]All the atomic charge densities for Cu and Ag used in this work are for the $\alpha = \frac{2}{3}$ potential. We thank Dr. J. T. Waber for providing us with these atomic charge densities.

[16]B. Segall, General Electric Research Laboratory Report No. 61-RL-2785G, 1961 (unpublished).

[17]Although the general d-band state involves the s and p components they are very insensitive to these components. The only states well below E_F for which these (mainly the s) components are important are the states around Γ_1, but these states do not appear to play an important role in any of the empirical information that we will be concerned with.

[18]The possibility of using this information to obtain the derivative of $\mathfrak{L}_1(E)$ is not too attractive since the derivative would be rather inaccurate.

[19]Shaw *et al.* (Ref. 8) have given an interpolation formula for obtaining the η_l at values of E_F other than those at which data were fitted.

[20]D. E. Eastman and J. K. Cashion, Phys. Rev. Lett. 24, 310 (1970).

[21]U. Gerhardt, Phys. Rev. 172, 651 (1968).

[22]P. O. Nilsson and B. Sandell, Solid State Commun. 8, 721 (1970).

[23]B. Segall and A. B. Chen (unpublished) (referred to as II throughout).

[24]H. Ehrenreich and H. R. Philipp, Phys. Rev. 128, 1622 (1962); E. L. Green and L. Mauldawer, Phys. Rev. B 2, 330 (1970); E. P. Pells (unpublished). We thank Dr. Pells for sending us his unpublished data.

[25]The relevant structure in Pells's unpublished ϵ_2 data extends from roughly $\hbar\omega = 5.45$ to 5.85 eV. The width of this structure is consistent with the calculated 0.3-eV spin-orbit splitting of the X_5 level (see Ref. 40) plus some broadening. Also, the magnitude of this structure is consistent with the corresponding $X_5 \rightarrow X_{4'}$ ϵ_2 structure in Pells and Shiga's Cu data (Ref. 39) when suitably scaled (according to ω^{-2}). The $X_5 \rightarrow X_{4'}$ transition in Cu is umambiguously identified by the piezo-optical response functions.

[26]The accuracy of the parametrized $v_0(E)$ is related to that of $v_2(E)$ through their connection at the L_1^u level [see step (e) in Sec. IV]. We suspect that the large error in Γ_1 is attributable to this effect combined with the large extrapolation.

[27]The quoted errors in Ref. 3 are: In the nonlinear fit, the rms errors are 0.0042 and 0.0045 Ry and the maximum errors are 0.0125 and 0.0132 Ry for Cu and Ag, respectively; in an alternative fit, the rms errors are 0.0041 and 0.0045 and the maximum errors are 0.0164 and 0.0172 Ry, respectively, for Cu and Ag. Dr. N. V. Smith informed us that the energy range they considered exceeded ours by only about 0.1 Ry.

[28]On the basis of the considerable experience gained in the last decade it is not difficult to construct a reason-

able potential. For example, one can construct the potential by the usual recipe of superposing atomic charge densities and potentials and including the local exchange-correlation correction with variable α. From the $E_n(\vec{k})$ corresponding to potentials for several α's, one can obtain a suitable value of α by interpolation.

[29]In the construction of this potential, we have used atomic charge densities corresponding to $\alpha = \frac{2}{3}$.

[30]The strong energy dependence of $v_l(E)$ for some of the extreme E_F values (see Table IV) indicates that relatively large errors may occur for the higher-energy states (see Sec. V). We note, however, that the $v_l(E)$ for the Ag $E_F = 0.35$ case are only weakly energy dependent. Nevertheless, appreciable differences from the level positions for $E_F = 0.75$ are found. Some of these differences are about four times larger than the expected errors.

[31]The main reason for these choices of E_F values is that they are the values within the plausible ranges at which Shaw *et al.* (Ref. 8) fitted the η_l's.

[32]J. F. Janak, A. R. Williams, and V. L. Moruzzi, Phys. Rev. B 6, 4367 (1972).

[33]A. R. Williams, J. F. Janak, and V. L. Moruzzi, Phys. Rev. Lett. 28, 671 (1972). Dr. Williams has informed us that the $E_n(\vec{k})$ that they calculated for the Chodorow potential are the same as those in Refs. 13 and 14 but that their E_F was slightly higher. As a consequence, the area of the neck of the Fermi surface (quoted in Ref. 32) is in better agreement with experiment.

[34]L. J. Sham and W. Kohn, Phys. Rev. 145, 561 (1966).

[35]V. L. Moruzzi, A. R. Williams, and J. F. Janak, Phys. Rev. B 9, 3316 (1974). We thank Dr. Williams for bringing this reference to our attention.

[36]This value is slightly different from that quoted in Ref. 33.

[37]I. Lindau and L. Wallden, Phys. Scr. 3, 77 (1971).

[38]N. V. Smith, Phys. Rev. B 3, 1862 (1971).

[39]G. P. Pells and M. Shiga, J. Phys. C 2, 1835 (1969).

[40]N. E. Christensen, Phys. Status Solidi (b) 54, 551 (1972).

[41]The average can be in error due to interaction effects from neighboring levels by roughly Δ_{so}^2/Δ_s, where Δ_{so} is the spin-orbit splitting and Δ is the separation from the neighboring level. Since $\Delta_{so} \sim 0.02$ Ry for Ag, this effect is very small unless $\Delta \lesssim 0.1$ Ry, which occurs only for the X_5 and X_2 levels.

[42]L. Wallden and T. Gustafson, Phys. Scr. 6, 73 (1972).

[43]This ratio is obtained from the calculations of Williams *et al.* (Ref. 33) for Cu, which should be approximately valid for Ag. We thank Dr. Williams *et al.* for the tabulation of matrix elements.

[44]The $R_l(r)$ out to the last inner node are very insensitive to the δV_l that will be encountered in these problems. In addition, the logarithmic derivative is specified at $r = r_i$. These two conditions impose reasonably strong constraints on the radial function at a given E.

[45]N. J. Coenen and A. R. Vroomen, J. Phys. F 2, 487 (1972), and the references therein.